ORGANIC LETTERS

2013
Vol. 15, No. 19
5040–5043

N-Heterocyclic Carbene Catalyzed Asymmetric Intermolecular Stetter Reaction: Origin of Enantioselectivity and Role of Counterions

Rositha Kuniyil and Raghavan B. Sunoj*

Department of Chemistry, Indian Institute of Technology Bombay, Powai, Mumbai 400076, India

sunoj@chem.iitb.ac.in

Received August 19, 2013

ABSTRACT

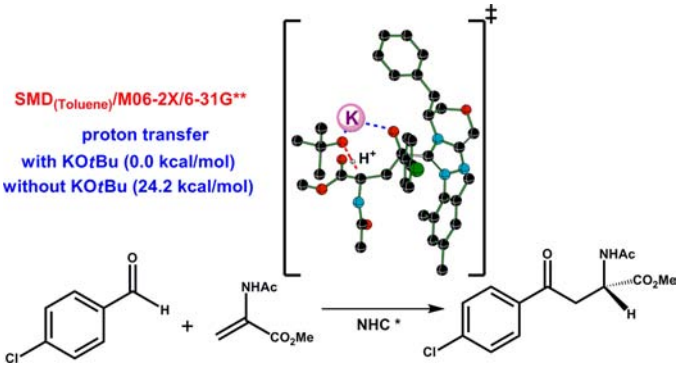

The mechanism and the role of KO*t*Bu in an enantioselective NHC-catalyzed Stetter reaction between *p*-chlorobenzaldehyde and *N*-acylamido acrylate is established using DFT(M06-2X) methods. The Gibbs free energies are found to be significantly lower for transition states with explicit bound KO*t*Bu as compared to the conventional pathways without the counterions. An intermolecular proton transfer from HO*t*Bu to the prochiral carbon is identified as the stereocontrolling step. The computed enantioselectivities are in excellent agreement with the experimental results.

The ability of N-heterocyclic carbenes (NHCs) to act as effective nucleophilic catalysts has been widely recognized in recent years.[1] A diverse range of NHC-catalyzed reactions are now available.[2] The current trends indicate an increasing interest in asymmetric applications of NHC catalysis, wherein the chiral induction is typically imparted by virtue of chiral centers present on the substituent arms attached to the nitrogen. Among the plethora of chiral NHC variants known to date, the triazolium family is one of the most widely used motifs in asymmetric synthesis.[3] In the repertoire of various NHC-catalyzed reactions, the asymmetric Stetter reaction is recognized as an effective protocol.[4]

(1) (a) Izquierdo, J.; Hutson, G. E.; Cohen, D. T.; Scheidt, K. A. *Angew. Chem., Int. Ed.* **2012**, *51*, 11686. (b) Vora, H. M.; Rovis, T. *Aldrichimica Acta* **2011**, *44*, 3. (c) Phillips, E. M.; Chan, A.; Scheidt, K. A. *Aldrichimica Acta* **2009**, *42*, 55. (d) Nair, V.; Vellath, S.; Babu, B. P. *Chem. Soc. Rev.* **2008**, *37*, 2691. (e) Enders, D.; Niemeier, O.; Henseler, A. *Chem. Rev.* **2007**, *107*, 5606. (f) Bugaut, X.; Glorius, F. *Chem. Soc. Rev.* **2012**, *41*, 3511.

(2) (a) Candish, L.; Lupton, D. W. *J. Am. Chem. Soc.* **2013**, *135*, 58. (b) Grossmann, A.; Enders, D. *Angew. Chem., Int. Ed.* **2011**, *50*, 7982. (c) Bugaut, X.; Liu, F.; Glorius, F. *J. Am. Chem. Soc.* **2011**, *133*, 8130. (d) De Sarkar, S.; Studer, A. *Org. Lett.* **2010**, *12*, 1992. (e) Mo, J.; Yang, R.; Chen, X.; Tiwari, B.; Chi, Y. R. *Org. Lett.* **2013**, *15*, 50. (f) Cohen, D. T.; Scheidt, K. A. *Chem. Sci.* **2012**, *3*, 53. (g) Wu, K.; Li, G. Q.; Li, Y.; Dai, Li.; You, S. *Chem. Commun.* **2011**, *47*, 493. (h) Thai, K.; Wang, L.; Dudding, T.; Bilodeau, F.; Gravel, M. *Org. Lett.* **2010**, *12*, 1992. (i) Lv, H.; Tiwari, B.; Mo, J.; Xing, C.; Chi, Y. R. *Org. Lett.* **2012**, *14*, 5412. (j) Grossmann, A.; Enders, D. *Angew. Chem., Int. Ed.* **2012**, *51*, 314. (k) Nair, V.; Vellalath, S.; Babu, B. P.; Varghese, V.; Paul, R. R.; Suresh, E. *J. Org. Chem.* **2010**, *8*, 4861. (l) Kawanaka, Y.; Phillips, E. M.; Scheidt, K. A. *J. Am. Chem. Soc.* **2009**, *131*, 18028. (m) Sun, L.-H.; Shen, L.-T.; Ye, S. *Chem. Commun.* **2011**, *47*, 10136.

(3) (a) Ryan, S. J.; Stasch, A.; Paddon-Row, M. N.; Lupton, D. W. *J. Org. Chem.* **2012**, *77*, 1113. (b) Ozboya, K. E.; Rovis, T. *Chem. Sci* **2011**, *2*, 1835. (c) Piel, I.; Steinmetz, M.; Hirano, K.; Frohlich, R.; Grimme, S.; Glorius, F. *Angew. Chem., Int. Ed.* **2011**, *50*, 4983. (d) He, M.; Struble, J. R.; Bode, J. W. *J. Am. Chem. Soc.* **2006**, *128*, 8418. (e) Raup, D. E. A.; Cardinal-David, B.; Holte, D.; Scheidt, K. A. *Nat. Chem.* **2010**, *2*, 766.

(4) (a) Domingo, L. R.; Zaragoza, R. J.; Saez, J. A.; Arno, M. *Molecules* **2012**, *17*, 1335. (b) Bortolini, O.; Fantin, G.; Fogagnolo, M.; Giovannini, P. P.; Massi, A.; Pacifico, S. *Org. Biomol. Chem.* **2011**, *12*, 1992. (c) Bhunia, A.; Yetra, S. R.; Bhojgude, S. S.; Biju, A. T. *Org. Lett.* **2012**, *14*, 2830. (d) Fang, X.; Chen, X.; Lv, H.; Chi, Y. R. *Angew. Chem., Int. Ed.* **2011**, *50*, 11827.

10.1021/ol402375d
Published on Web 09/13/2013

The generally proposed mechanism in these reactions involves the addition of a Breslow intermediate to suitable electrophiles. Depending on the nature of the reactions, different transition state models are reported in literature that help rationalize the vital facial discrimination responsible for asymmetric induction.[5] However, when the stereocontrolling step involves a protonation, the mechanistic picture tends to become more vague owing to the near isosteric prochiral faces offered by the substrate to the incoming proton. It is therefore of inherent interest to identify the stereocontrolling factors in the enantioselective protonation reactions. The intermolecular Stetter reaction, reported by Glorius and co-workers, provides an effective and milder route toward enantioenriched α-amino acids (Scheme 1). Herein, we report the origin of stereoselectivity and the role of counterions besides the mechanism of the title reaction.

Scheme 1. Stetter Reaction of *p*-Chlorobenzaldehyde with *N*-Acylamido Acrylate[8]

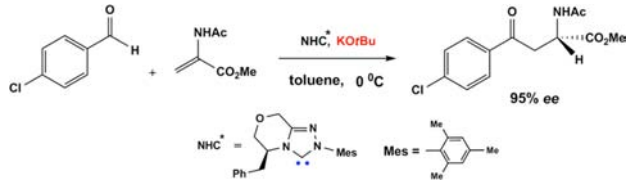

As a part of our interest toward understanding the origin of stereoselectivity[6] and the role of counterion in organocatalytic reactions, we have investigated the role of KO*t*Bu in a chiral triazolium-catalyzed Stetter reaction between *p*-chlorobenzaldehyde and N-acylamido acrylate. The M06-2X/6-31G** density functional theory, including the effect of solvent (toluene, as used in the experiments), is employed for full geometry optimization of all transition states (TSs) and intermediates. The discussions are presented on the basis of the Gibbs free energies obtained at the $SMD_{(Toluene)}$/M06-2X/6-31G** level of theory.[7]

A closer examination of the experimental conditions reveals that the presence of a strong base such as KO*t*Bu is critical to the success of the reaction.[8] While the base is proposed to participate in the generation of free NHC from its precursor, additional roles of the same cannot be ignored. Akin to the mechanistic proposals reported earlier, we have considered a number of pathways in the present study. These differ primarily in regards to the explicit participation of KO*t*Bu in the key TSs of the reaction. The mechanism of the reaction can be considered as consisting of the following key events, as shown in Scheme 2.

Scheme 2. Mechanistic Steps Involved in Asymmetric Stetter Reaction

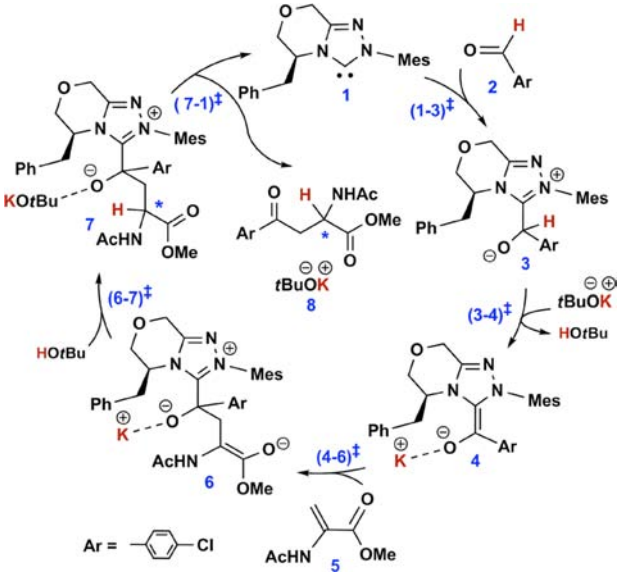

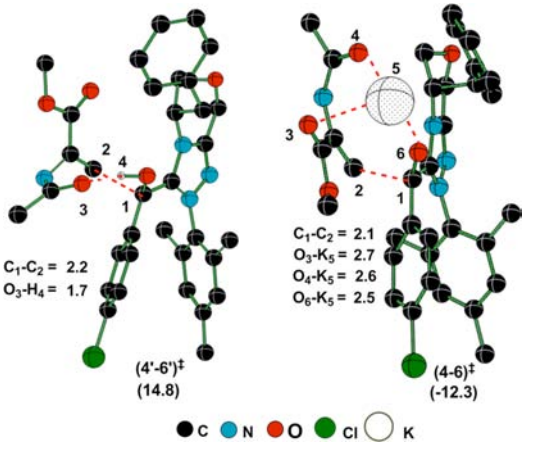

Figure 1. Lower energy transition states for C−C bond fomation with and without potassium coordination obtained at the $SMD_{(Toluene)}$/ M06-2X/6-31G** level. Bond lengths are given in Å.

The initial addition of NHC (**1**) to the aryl aldehyde (**2**, *p*-chlorobenzaldehyde) via **(1−3)**‡ results in a zwitterionic intermediate **3**. It has been reported that the generation of the Breslow intermediate (enaminol) could involve significant barriers unless a base-assisted proton transfer mechanism is invoked.[9,6b] In view of this, an active role for KO*t*Bu is envisaged wherein the potassium ion is bound to

(5) (a) Zhang, W.; Zhu, Y.; Wei, D.; Li, Y.; Tang, M. *J. Org. Chem.* **2012**, *77*, 10729. (b) Lyngvi, E.; Bode, J. W.; Schoenebeck, F. *Chem. Sci.* **2012**, *3*, 2346. (c) Domingo, L. R.; Zaragoza, R. J.; Saez, J. A.; Arno, M. *Molecules*. **2012**, *13*, 1335. (d) He, Y.-Q.; Xue, Y. *J. Phys. Chem.* **2011**, *115*, 1408.

(6) (a) Sharma, A. K.; Sunoj, R. B. *Angew. Chem., Int. Ed.* **2010**, *49*, 6373. (b) Reddi, Y.; Sunoj, R. B. *Org. Lett.* **2012**, *14*, 2810. (c) Sreenithya, A.; Sunoj, R. B. *Org. Lett.* **2012**, *14*, 5752. (d) Sharma, A. K.; Sunoj, R. B. *J. Org. Chem.* **2012**, *77*, 10516. (e) Jindal, G.; Sunoj, R. B. *Chem.—Eur. J.* **2012**, *18*, 7045.

(7) (a) Additional conformational as well as mechanistic possibilities are examined using the $SMD_{(Toluene)}$/M06-2X/6-31G**//B3LYP/6-31G** level of theory. (b) All computations were carried out using the Gaussian 09 program. Frisch, M. J. et al. *Gaussian 09*, revision A.02; Gaussian, Inc.: Wallingford, CT, 2004. More details are in the Supporting Information (SI).

(8) Jousseaume, T.; Wurz, N. E.; Glorius, F. *Angew. Chem., Int. Ed.* **2011**, *50*, 1410.

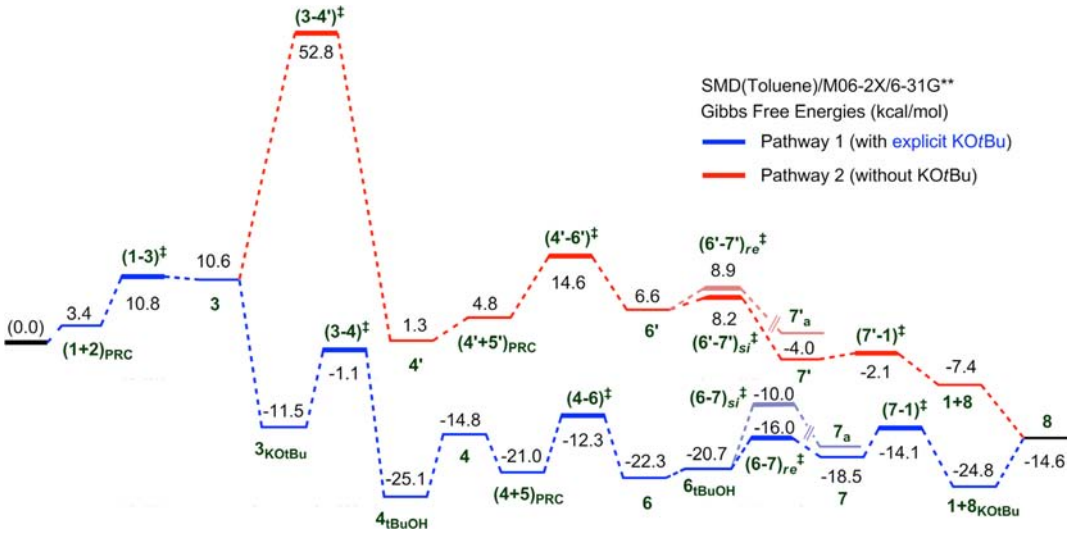

Figure 2. Gibbs free energy profile for pathways 1 and 2 involved in the formation of enantioenriched α-amino acids.

the alkoxide oxygen while the butoxide counterion is hydrogen bonded to the benzylic proton.[10] Complete abstraction of the benzylic proton and the ensuing expulsion of HO*t*Bu provides a potassium enolate intermediate **4**. In the next vital step, the addition of **4** to the Michael acceptor (*N*-acylamido acrylate **5**) through **(4**−**6)**‡ results in the C−C bond formation. The enolate intermediate **6** thus formed can undergo a stereoselective intermolecular protonation at the prochiral carbon atom to furnish intermediate **7**. In the last step, the expulsion of NHC from **7** provides product **8** bound to KO*t*Bu.

First, the energies of different conformers of *N*-acylamidoacrylate are examined to identify that a *syn* disposition of the acyl carbonyl and the olefin are much more favored than six other higher energy conformers.[11] Two lower energy conformers, within a range of 2 kcal/mol, are considered in the ensuing steps of the reaction. In the C−C bond formation TS, namely **(4**−**6)**‡, both *E* and *Z* configurations of the Breslow intermediate as well as different conformers arising due to the differences in the relative orientations of the *N*-acyl group with respect to the aryl group are as well examined.[12] In the most preferred TS for the C−C bond formation, as shown in Figure 1, the potassium ion plays an anchoring role by binding to the oxygen atoms of the incoming Michael acceptor and that of the Breslow intermediate. In this TS, the N-acyl moiety is *anti* to the aryl group of the substrate. In all other TSs wherein *N*-acyl is *syn* to the substrate aryl group, the energies are found to be more than 5 kcal/mol higher.

The next important mechanistic event is the protonation at the prochiral carbon atom. Different modes of protonations are envisaged. For instance, in the absence of an explicitly bound potassium ion, an intramolecular proton transfer from the hydroxyl group to the prochiral carbon (in the intermediate equivalent to **6**) is the stereocontrolling step.[13] A significant aspect that merits comparison at this juncture is the energetics of the reaction, in the presence and absence of KO*t*Bu. The comparison of the Gibbs free energy profiles for pathways 1 and 2, respectively with and without KO*t*Bu, conveys that the TSs in Pathway 2 are of higher energy (Figure 2). In particular, steps leading to the Breslow intermediate and C−C bond formation are respectively 54 and 27 kcal/mol higher in energy in the absence of KO*t*Bu. More importantly, the stereocontrolling protonation TS **(6**−**7)**‡ in Pathway 1 is lower by 24 kcal/mol.

In Pathway 1, a favorable intermolecular proton transfer from HO*t*Bu is identified as being responsible for the observed enantioselectivity. Different modes of intermolecular protonation on the prochiral faces of enolate **6** are examined. The geometries as well as the Gibbs free energies of the two lowest energy diastereomeric transition states for protonation, namely $\mathbf{(6-7)}^{\ddagger}_{re}$ and $\mathbf{(6-7)}^{\ddagger}_{si}$, are provided in Figure 3. It can be noticed that the protonation on the *re*-face is relatively more preferred over that on the *si*-face. $\mathbf{(6-7)}^{\ddagger}_{re}$, wherein the potassium ion simultaneously interacts with the alkoxide and the ester oxygens, is found to be the most preferred protonation TS.

(9) (a) Verma, P.; Patni, P. A.; Sunoj, R. B. *J. Org. Chem.* **2011**, *76*, 5606. (b) In the present example, the computed barrier for 1,2-proton transfer in **3** to furnish the Breslow intermediate is found to be 52.8 kcal/mol.

(10) (a) The optimized geometries of KO*t*Bu-assisted formation of Breslow intermediate **(3**−**4)**‡ is given in Figure S6 in the SI.

(11) (a) The other conformers are found to be higher by 5.6 to 7.6 kcal/mol than the lowest energy conformer at the $SMD_{(Toluene)}$/M06-2X/6-31G**//B3LYP/6-31G** level of theory. (b) See Figure S1 in the SI for additional details on the conformers.

(12) (a) The energies of the TSs involving the *Z* isomer is in general higher in energy by 4 kcal/mol. (b) Details of additional TSs with and without the potassium coordination are provided respectively in Tables S1 and S3 in the SI.

(13) (a) The energies of all intramolecular and intermolecular proton transfer TSs are respectively given in Figures S6 and S3 in the SI.

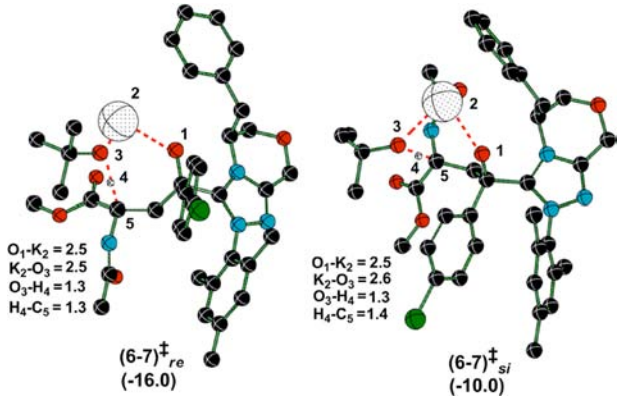

Figure 3. Lower energy transition states for stereoselective proton transfer on the *re*- and *si*-faces of enolate **6** at the $SMD_{(Toluene)}$/M06-2X/6-31G** level. The relative Gibbs free energies (kcal/mol) are given in parantheses. Bond lengths are in Å. Only selected hydrogens are shown for improved clarity.

Careful analysis of these stereocontrolling TSs is carried out to identify the stereoelectronic factors that control the energy difference between $(\mathbf{6-7})^{\ddagger}_{re}$ and $(\mathbf{6-7})^{\ddagger}_{si}$. The atoms-in-molecule (AIM) and Natural Bond Orbital (NBO) analyses revealed the differential stereoelectronic features in these competing TSs.[14] For instance, the electrostatic interaction between the O^- of the CO_2Me group and K^+ imparts additional stabilization in $(\mathbf{6-7})^{\ddagger}_{re}$, which is absent in $(\mathbf{6-7})^{\ddagger}_{si}$. Moreover, the number of $C-H\cdots\pi$ interactions in the lower energy $(\mathbf{6-7})^{\ddagger}_{re}$ are found to be more prominent than in $(\mathbf{6-7})^{\ddagger}_{si}$. The overall electron delocalization between the reacting partners is estimated to be higher in the case of $(\mathbf{6-7})^{\ddagger}_{re}$ than in $(\mathbf{6-7})^{\ddagger}_{si}$.[14b]

(14) (a) An exhasutive mapping of all intramolecular stabilizing contacts in $(\mathbf{6-7})^{\ddagger}_{re}$ and $(\mathbf{6-7})^{\ddagger}_{si}$ is provided in Table S6 in the SI. (b) Donor–acceptor orbital interactions between the reacting fragments is computed as the second-order perturbation energies using NBO analysis. Additional details are provided in Table S5 in the SI.

The computed energy difference between the diastereomeric TSs $(\mathbf{6-7})^{\ddagger}_{re}$ and $(\mathbf{6-7})^{\ddagger}_{si}$ is 6.1 kcal/mol, which corresponds to an enantiomeric excess of >99% in favor of the *S* isomer. This prediction is in good accordance with the experimentally observed *ee* of 95%. Another key observation that emerged through the present study is the inability of the TS models without explicit KO*t*Bu to predict the formation of the correct enantiomeric product.[15] In fact, in the absence of KO*t*Bu, $(\mathbf{6-7})^{\ddagger}_{si}$ is identified as more preferred, leading to an erroneous estimate on the stereochemical outcome of the reaction.

In conclusion, the enantioselectivity in the NHC-catalyzed Stetter reaction between *p*-chlorobenzaldehyde and *N*-acylamido acrylate is identified to be controlled by an intermolecular protonation by HO*t*Bu. The reaction energetics are predicted to be much more favorable when KO*t*Bu is explicitly included in the transition states as compared to the generally suggested mechanism.

Acknowledgment. Computing time from the IIT Bombay supercomputing facility is gratefully acknowledged. We thank the Industrial Research and Consultancy Center (IRCC), IIT Bombay for financial support through 12IRAWD005. R.K. acknowledges fruitful discussions with Yernaidu Reddi, Garima Jindal, and A. Sreenithya (Computational Chemistry Lab, IIT Bombay).

Note Added after ASAP Publication. The TOC/abstract graphic contained errors in the version published ASAP on September 13, 2013; the correct version reposted September 16, 2013.

Supporting Information Available. Details of computational methods, complete citation for ref 7b, and optimized geometries of the stationary points are provided. This material is available free of charge via the Internet at http://pubs.acs.org.

(15) The details of energetics associated with the mechanism in the absence of KO*t*Bu (Figure S4) is provided in Table S4 in the SI.

The authors declare no competing financial interest.